racy of ±5% or better in the composition range between 0.1 and 0.9 volume fractions. This accuracy is sufficient for most engineering calculations and could be increased by improving the instrumentation and providing a better mixing section. The major advantage of the flow calorimeter is that it can be easily modified to operate at elevated pressure.

The flow calorimeter has two distinct disadvantages. It requires a large quantity of pure components which are usually difficult and expensive to obtain. In addition, the precision of the measurements is least reliable at low concentrations, the very region where precision data would be most valuable for comparison with the theories of liquid structure. Although design improvements can reduce these errors, very high precision batch or semibatch calorimeters will be required to eliminate both of these shortcomings. Such an instrument has been perfected by Van Ness and coworkers (*4*, *9*).

ACKNOWLEDGMENT

The authors acknowledge the graduate fellowship support received from the Texaco Co. and the Shell Oil Co. Financial assistance from the Engineering Experiment Station at the University of Missouri provided special equipment and the chemicals required for this project.

NOMENCLATURE

ΔH = heat of mixing, joules/cc., joules/mass
V = molar volume, cc./g.-mole
x = mole fraction
ϕ = volume fraction
ρ = density, g./ml., g. mole/cc.

SUBSCRIPTS

1 = alcohol
2 = hydrocarbon solvent

LITERATURE CITED

(1) Brown, I., Fock, W., *Australian J. Chem.* **14**, 387 (1961).
(2) Brown, I., Fock, W., Smith, F., *Ibid.*, **17**, 1106 (1964).
(3) "International Critical Tables," Vol. **5**, p. 86, McGraw-Hill, New York, 1929.
(4) Mrazek, R.V., Van Ness, H.C., *A.I.Ch.E. J.* **7**, 190 (1961).
(5) Mueller, C.R., Lewis, J.E., *J. Chem. Phys.* **25**, 1166 (1956).
(6) Pratt, F.R., *J. Franklin Inst.* **185**, 663 (1918).
(7) Rose, V.C., Ph.D. dissertation, University of Missouri, January 1965.
(8) Rossini, F.D., ed., "Experimental Thermochemistry," pp. 237–86, Interscience, New York, 1956.
(9) Savini, C.G., Winterhalter, D.R., Van Ness, H.C., J. CHEM. ENG. DATA **10**, 168 (1965).
(10) Sieg. L., *Chem.-Eng.-Tech.* **23**, 112 (1951).
(11) Skinner, H.A., ed., "Experimental Thermochemistry," Wiley, New York, 1962.
(12) Weissberger, A., ed., "Physical Methods of Organic Chemistry," 3rd ed., Part I, Interscience, New York, 1959.
(13) White, W.P., "Modern Calorimeter," Chemical Catalog Co., New York, 1928.

RECEIVED for review October 5, 1964. Accepted November 26, 1965.

Isobaric Vapor-Liquid Equilibrium of *n*-Heptane–*n*-Butanol System

S. V. VIJAYARAGHAVAN, P. K. DESHPANDE, and N. R. KULOOR
Department of Chemical Engineering, Indian Institute of Science, Bangalore-12, India

Vapor-liquid equilibrium data for the system *n*-heptane–*n*-butanol have been reported. The thermodynamic consistency of the data was tested with Chao's modified Redlich-Kister equation and Tao's method.

VAPOR-LIQUID equilibrium data for the system *n*-heptane–*n*-butanol are available only at isothermal conditions (*6*). Therefore, the system has been studied under isobaric conditions at 684 ± 5 mm. of Hg.

EXPERIMENTAL

The equilibrium still used has been described (*8*), and it is a modified Ellis and Garbett (*2*) still. The still was operated without stirrers for 3 hours to attain equilibrium, and then samples were drawn for analysis.

Both *n*-heptane and *n*-butanol of British Drug House laboratory reagent grade were used. The density and refractive index of reagents and also the literature values are given in Table I.

Samples were analyzed by determination of density and viscosity. The viscosity was determined using Hoppler's falling ball viscometer. A calibration chart was initially constructed from the data of known composition.

THERMODYNAMIC CONSISTENCY

The experimental vapor-liquid equilibrium data are presented in Table II. Liquid phase activity coefficients are calculated from the equation,

Table I. Properties of Pure Components

	Density, at 20° C.		Refractive Index, at 20° C.	
Compound	Exptl.	Lit. (*3*)	Exptl.	Lit. (*3*)
1. *n*-Heptane	0.68380	0.68376	1.3880	1.3876
2. *n*-Butanol	0.80986	0.80978	1.3988	1.3991

Table II. Vapor-Liquid Equilibrium Data (Pressure 684 ± 5 mm.)

		Mole % of *n*-Heptane			
No.	Temp., ° C.	Liquid	Vapor	γ_1	γ_2
1	103.8	5.7	37.0	4.995	1.007
2	98.2	14.2	54.4	3.469	1.013
3	95.2	22.1	62.1	2.790	1.043
4	92.2	32.9	69.3	2.282	1.108
5	90.2	43.4	73.0	1.941	1.259
6	89.5	55.2	75.8	1.622	1.471
7	89.0	61.4	77.4	1.510	1.627
8	88.8	73.8	79.5	1.296	2.190
9	89.3	91.1	84.6	1.100	4.984
10	93.4	98.0	93.5	1.001	7.532

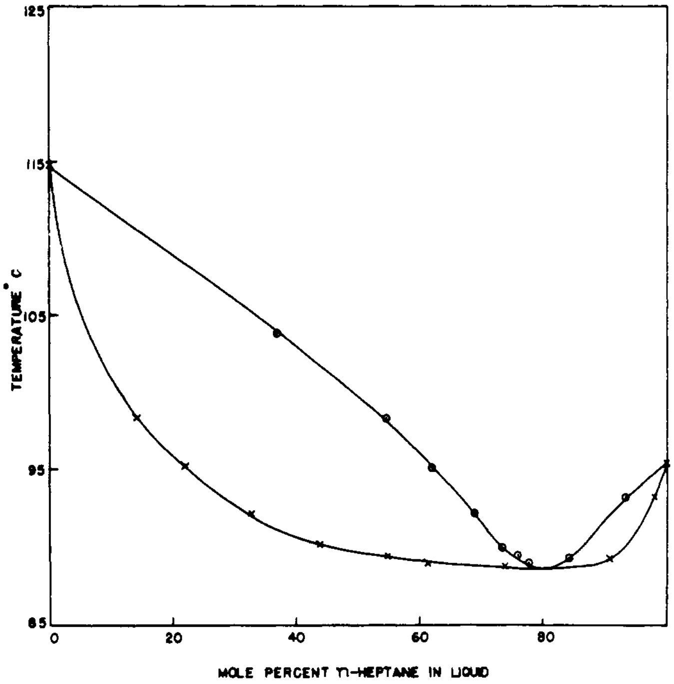

Figure 1. *t-x-y* Diagram at 684 mm. of Hg
System: *n*-heptane–*n*-butanol

$$\gamma_i = \frac{y_i P}{x_i P_i^\circ} \theta_i \tag{1}$$

assuming the vapor imperfection coefficient, θ_i to be 1.

The vapor pressures for various temperatures are calculated from the following equation (3):

$$n\text{-heptane: } \log_{10} p^\circ \text{ (mm.)} = 6.90319 - \frac{1268.586}{216.954 + t} \tag{2}$$

$$n\text{-butanol: } \log_{10} p^\circ \text{ (mm.)} = \frac{-52.23 \times 46.774}{T} + 9.1362 \tag{3}$$

The *t-x-y* diagram showed that the system is a minimum boiling point type and forms an azeotrope at 80.7 mole % of *n*-heptane (Figures 1 and 2).

The thermodynamic consistency of the data obtained was tested by Tao's method (7). For this, dimensionless excess free energy, Q, and dimensionless thermodynamic function, α, are calculated from experimental data with the help of the following equations:

$$Q = \sum_i x_i \ln \gamma_i = Q_e \tag{4}$$

$$\alpha_1 = A(x_1) + B(x_1) + \ln \frac{\gamma_1}{\gamma_2} \quad \text{(for binary system)} \tag{5}$$

where

$A(x_1) = -(H/RT^2)(dT/dx)$ (assumed negligible in the present case)

$B(x_1) = -(V/RT)(dP/dx)$ (equal to zero, since the data are at isobaric condition)

$$Q\Big|_{x_{1_s}} - Q\Big|_{x_{1_r}} = \int_{x_{1_r}}^{x_{1_s}} \alpha_1 dx_1 = \Delta Q_c \tag{6}$$

and

$$\alpha_1 = dQ/dx_1 = \alpha_{1_c} \tag{7}$$

where subscripts r and s denote any two points on the path under consideration. Q and α_1 can also be obtained indirectly from Equations 6 and 7.

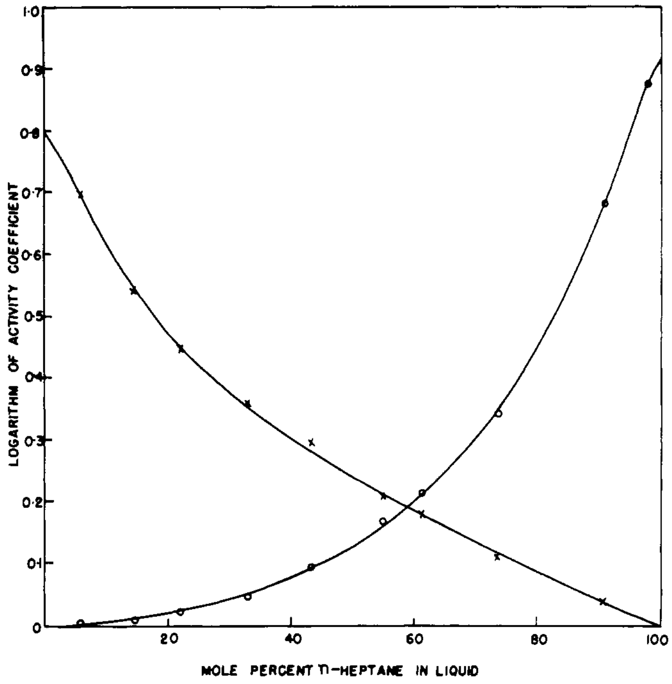

Figure 2. Logarithm of the activity coefficient *vs.* composition
System: *n*-heptane–*n*-butanol

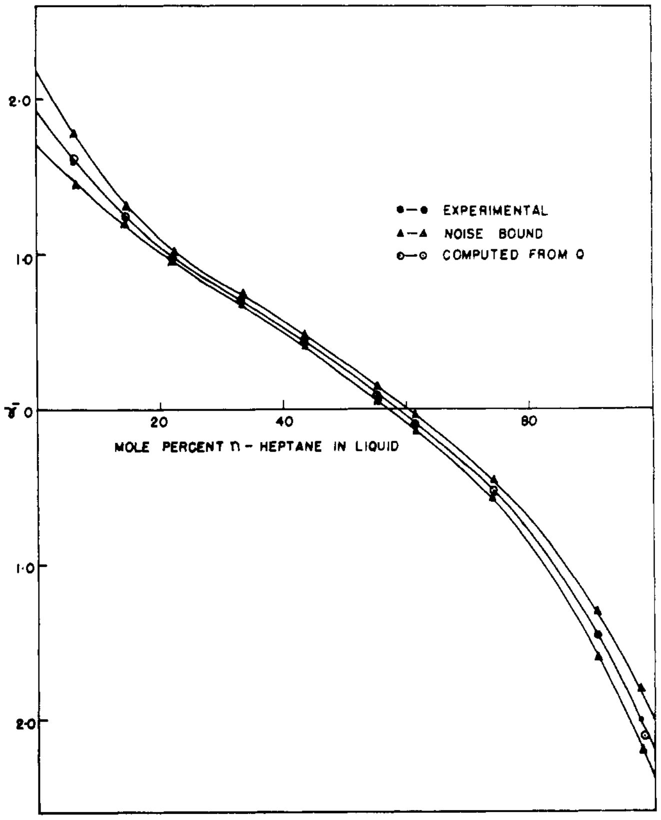

Figure 3. γ_1 *vs.* composition
System: *n*-heptane–*n*-butanol

Since all experiments will have noise, the noise bounds are calculated from the knowledge of maximum errors in the measurement of temperature, $E(T)$; pressure, $E(T)$; and composition, $E(x)$. The propagation of these errors to the computed thermodynamic quantities can be calculated from Equations 8, 9, and 10, which are derived by taking total derivatives of Equations 1, 4, and 5, not including θ_i, A, and B.

$$\frac{E(\gamma_i)}{\gamma_i} = E(P)/P + [E(T)/p_i^\circ]\,[dp_i^\circ/dT] + [(1/y_i) + (1/x_i)]\,E(x) \qquad (8)$$

$$E(Q) = \sum_i \left[x_i \frac{E(\gamma_i)}{\gamma_i} + E(x) \ln \gamma_i \right] \qquad (9)$$

$$E(\alpha_1) = \frac{E(\gamma_1)}{\gamma_1} - \frac{E(\gamma_2)}{\gamma_2} \qquad (10)$$

The maximum errors of measurement are $E(T) = 0.05$, $E(P) = 0.5$, and $E(x) = 0.01$. The values of α_{1_e} are plotted against x_i in Figure 3 along with the noise bounds and calculated α_{1_c}. This figure shows that calculated values of thermodynamic functions α_1 are within the noise bounds which indicates local as well as over-all consistency of the data.

The thermodynamic consistency of the data was also tested using Chao's (*1*) modified Redlich-Kister equation. The values of constants in the equation,

$$\log \frac{\gamma_1}{\gamma_2} = a + b(x_2 - x_1) + c(6x_1x_2 - 1) + d(x_2 - x_1)\,(1 - 8x_1x_2) \qquad (11)$$

are $a = 0.048$, $b = 0.730$, $c = 0.096$, and $d = 0.130$.

The area test of Redlich-Kister (*5*) is satisfactory, and the calculated values of log γ_1/γ_2 from Equation 11 are in good agreement with experimental values. Herington's test (*4*) for consistency is also satisfactory since experimental $D\text{-}J = 4.74 < 10$.

NOMENCLATURE

a, b, c, d = constants in Chao's equation
A, B = defined functions in Equation 5
E = error
H = integral heat of mixing
P = total pressure
p° = vapor pressure of pure component
Q = dimensionless excess free energy
R = gas constant
T = absolute temperature
V = integral volume change of mixing
x = mole fraction of component in liquid phase
y = mole fraction of component in vapor phase
γ_1 = dimensionless thermodynamic function in Equations 5 and 7
γ = liquid activity coefficient
θ_i = vapor imperfection coefficient

Subscripts

r, s = points on a linear path
i = component identity
c = computed indirectly from data
e = computed directly from experimental results
1 = *n*-heptane
2 = *n*-butanol

LITERATURE CITED

(1) Chao, K.C., Hougen, O.A., *Chem. Eng. Sci.* **7**, 246 (1958).
(2) Ellis, S.R.M., Garbett, R.D., *Ind. Eng. Chem.* **52**, 385 (1960).
(3) "Handbook of Chemistry and Physics," 44th ed., Charles D. Hodgman, Ed., Chemical Rubber Publishing Co., Cleveland, Ohio, 1962-63.
(4) Herington, E.F.G., *J. Inst. Petrol.* **37**, 457 (1951).
(5) Redlich, O., Kister, A.T., *Ind. Eng. Chem.* **40**, 345 (1948).
(6) Smyth, C.P., Engel, E.W., *J. Am. Chem. Soc.* **51**, 2660 (1929).
(7) Tao, L.C., *Ind. Eng. Chem.* **56**, 36 (1964).
(8) Vijayaraghavan, S.V., Deshpande, P.K., Kuloor, N.R., *Indian J. Tech.* **2**, 249 (1964).

RECEIVED for review October 5, 1964. Accepted February 9, 1966.

Transient Solute Concentrations and Phase Changes of Calcium Sulfate in Aqueous Sodium Chloride

WILSON H. POWER and BELA M. FABUSS
Monsanto Research Corporation, Everett, Mass.

CHARLES N. SATTERFIELD
Massachusetts Institute of Technology, Cambridge, Mass.

The change in solute concentration with time of 0.25*m* or 1.0*m* NaCl in contact with gypsum, β-hemihydrate, β-soluble anhydrite, or insoluble anhydrite was determined over the temperature range of 25° to 105° C. Accompanying changes in the solid phase were also determined. Under thermodynamically favorable conditions, β-hemihydrate and β-soluble anhydrite rapidly hydrate to form gypsum. The dehydration rate of gypsum at 95° and 105° C. to form insoluble anhydrite is much faster in 1.0*m* NaCl than in pure water. Some changes in solubility and solid phase composition occur only after an induction period of 2 days or more. Solubility product constants for gypsum and insoluble anhydrite agree closely with previously published values. From present data and earlier literature values, a correlation is presented for estimating the solubility of gypsum and anhydrite over a wide range of ionic strength.

AN EARLIER PAPER (*7*) reported on the change in solute concentration of water with time in contact with α- or β-calcium sulfate hemihydrate, β-soluble anhydrite, or insoluble anhydrite. The changes in solute concentration were related to changes in the nature of the calcium sulfate solid phase present. The present study extends the earlier work to an investigation of the transient behavior of various forms of calcium sulfate in contact with aqueous sodium chloride solutions.

Measurements were carried out in a 1-liter borosilicate glass flask, and the experimental method was as previously described except that in the presence of sodium chloride, conductivity could not be used to determine calcium sulfate solubility as before. Instead, solutions were analyzed for